# Oscillatory instability of radiative shocks with multiple cooling processes

Curtis J. Saxton,[1,2] Kinwah Wu,[1] Helen Pongracic[3] and Giora Shaviv[4]

[1]*Special Research Centre for Theoretical Astrophysics, School of Physics, University of Sydney, NSW 2006, Australia*
[2]*Sir Frank Packer Department of Theoretical Physics, School of Physics, University of Sydney, NSW 2006, Australia*
[3]*Air Operations Division, Aeronautical and Maritime Research Laboratory, Defence Science and Technology Organisation, VIC 3001, Australia*
[4]*Asher Space Research Institute and Department of Physics, Technion, Haifa 32000, Israel*

**ABSTRACT**
The stand-off shock formed in the accretion flow on to a stationary wall, such as the surface of a white dwarf, may be thermally unstable, depending on the cooling processes which dominate the post-shock flow. Some processes lead to instability, while others tend to stabilize the shock. We consider competition between the destabilizing influence of thermal bremsstrahlung cooling, and a stabilizing process which is a power law in density and temperature. Cyclotron cooling and processes which are of order 1, 3/2 and 2 in density are considered. The relative efficiency and power-law indices of the second mechanism are varied, and particular effects on the stability properties and frequencies of oscillation modes are examined.

**Key words:** accretion, accretion discs – shock waves – binaries: close – white dwarfs.

## 1 INTRODUCTION

Radiative shocks are thermally unstable for certain cooling laws, and are thereby driven to oscillate, giving rise to variabilities of radiation emitted from the shock-heated matter. This phenomenon occurs in a wide range of astrophysical situations, ranging from supernova remnants to accreting compact objects. Time-dependent properties of radiative shocks have been investigated by various authors (e.g. Falle 1975, 1981; Langer, Chanmugam & Shaviv 1981, 1982; Chevalier & Imamura 1982; Imamura, Wolff & Durisen 1984; Chanmugam, Langer & Shaviv 1985; Imamura 1985; Bertschinger 1986; Innes, Giddings & Falle 1987a, b; Gaetz, Edgar & Chevalier 1988; Wolff, Gardner & Wood 1989; Imamura & Wolff 1990; Houck & Chevalier 1992; Wu, Chanmugam & Shaviv 1992; Tóth & Draine 1993; Dgani & Soker 1994; Imamura et al. 1996; Saxton, Wu & Pongracic 1997). The stability properties of the radiative shocks depend on the cooling processes and the boundary conditions subject to which the shocks are formed. In this paper we will investigate the stability properties of radiative shocks, using a planar model with appropriate cooling processes and boundary conditions appropriate for accreting magnetic white dwarfs.

For accretion on to white dwarfs, a stand-off shock is formed near the white dwarf surface when the supersonic accretion matter decelerates abruptly to a subsonic flow. The height of the shock above the white dwarf surface can be estimated from the cooling path-length, which is approximately $h = v_{ff} t_{cool}/4$, where $v_{ff}$ is the free-fall velocity at the white dwarf surface, and $t_{cool}$ is the cooling time-scale. For parameters typical of cataclysmic variables (see Warner 1995), which are low-mass close binaries containing a red dwarf transferring matter to a white dwarf, the major cooling process is bremsstrahlung radiation if the white dwarf magnetic field is weak ($\lesssim 10$ MG), and cyclotron radiation if the field is strong ($\gtrsim 10$ MG) (e.g. King & Lasota 1979; Lamb & Masters 1979). As bremsstrahlung and cyclotron cooling have different density and temperature dependence, their effects on the stability of the shocks will be different.

Time-dependent accretion on to white dwarfs, with planar geometry, was first investigated by Langer et al. (1981). Their numerical studies showed that if bremsstrahlung is the only cooling process, the accretion shocks are thermally unstable, thus giving rise to quasi-periodic oscillations. Linear analyses with bremsstrahlung cooling were carried out by Chevalier & Imamura (1982), and it was shown that the fundamental mode of the shock oscillation is stable, but that the overtones are unstable. Chevalier & Imamura also considered a general situation in which the total cooling process is represented by a single cooling function with power laws of density $\rho$ and temperature $T$. (Thus $\Lambda \propto \rho^a T^b$, where $a$ and $b$ are the power-law indices. For bremsstrahlung cooling, $a = 2$ and $b = 0.5$.) Their analyses showed that cooling functions with a higher power dependence on the temperature tend to stabilize the shock and hence suppress the shock oscillations.

Stability of radiative shocks in spherical geometry was investigated by Bertschinger (1986). In these calculations, the total cooling is again represented by a single cooling function with power laws of density and temperature. Both radial perturbations and transverse perturbations, which are expressed in terms of a scaled transverse wavenumber in addition to the usual oscillation frequency, were considered. It was found that the oscillatory modes which are stable to purely radial perturbations (those stable in the limit of the results of Chevalier & Imamura 1982) are destabilized for non-radial perturbations over some range of wavenumber. For indefinitely great wavenumber all modes were eventually and increasingly stabilized.

Radial accretion on to compact objects, with a Newtonian gravitational potential, was investigated by Houck & Chevalier (1992). In their calculations, a single cooling function of power laws in density and temperature was used, and cases with different adiabatic index and power-law indices were considered. Their calculations reproduced the results of Chevalier & Imamura (1982), and additionally showed that appreciable spherical extension of the post-shock region, even with a very mild curvature, tends to destabilize the first and second harmonics whilst higher order modes are stabilized, with the damping being stronger for higher harmonics.

Dgani & Soker (1994) considered situations that allow mass-loss in the post-shock flow. A mass-loss term was introduced in the continuity equation to take into account the transverse flow of material in physically extended shocks. For a variety of single power-law-type cooling functions, mass-loss stabilizes shock oscillations. Its effect is weaker when the power-law index for the temperature is smaller.

Tóth & Draine (1993) investigated the stability of shocks supported by a transverse magnetic field. In their work the oscillatory stability was determined by support from the magnetic field lines, rather than the functional properties of radiative cooling processes.

Imamura et al. (1996) investigated the stability of an accretion shock with unequal electron and ion temperatures, and the effects of Compton and bremsstrahlung cooling are included. They considered both the longitudinal perturbations and the transverse perturbations. This work is applicable to systems where the electron–ion energy exchange time-scale is comparable to or longer than the radiative cooling time-scale. They found that the two-temperature effects increase the oscillatory instability of the shock, for both the radial and non-radial modes. Stability properties of transverse and radial modes are similarly affected by changes in the temperature index of the single power-law cooling process.

In all the studies mentioned above, the total cooling is represented by a single cooling function. In realistic systems, cooling processes are independent: some processes (e.g., bremsstrahlung cooling) destabilizes the shock oscillations, while other processes (e.g., cyclotron cooling) have stabilizing effects. Radiative shocks with more than one cooling process are complicated, and their stability properties can be determined only when all these processes are treated explicitly.

Numerical simulations of accretion on to magnetic white dwarfs, with explicit treatment of both bremsstrahlung and cyclotron cooling, were first carried out byChanmugam et al. (1985). Their study showed that the presence of cyclotron cooling tends to suppress the shock oscillations. Later simulations by Wu et al. (1996) showed that the suppression is efficient only when the magnetic field is sufficiently strong. Small-amplitude oscillations persist if the field is weak ($\lesssim 10$ MG). When bremsstrahlung and cyclotron cooling have similar strengths, the oscillation is a two-phase process, with bremsstrahlung cooling dominating during one part of the cycle and cyclotron cooling during the other (Wu et al. 1992).

Saxton et al. (1997) carried out a linear perturbative stability analysis for planar accretion shocks with bremsstrahlung and cyclotron cooling. They considered a composite cooling function in which there is a bremsstrahlung cooling term ($\Lambda_{\mathrm{br}} \propto \rho^2 T^{0.5}$) and an effective cyclotron cooling term ($\Lambda_{\mathrm{cy}} \propto \rho^{0.15} T^{2.5}$). The relative efficiency of the cyclotron cooling varies with the magnetic field strength. Cases with different relative strength of cyclotron cooling were considered. Their analyses showed that lower harmonics were successively stabilized as cyclotron strength increased.

In this work we extend the analyses of Saxton et al. (1997) to a generalized composite cooling function, consisting of the bremsstrahlung term and a second power-law cooling term ($\Lambda_2 \propto \rho^a T^b$), which replaces the earlier approximate cyclotron term. We vary the power-law indices $a$ and $b$, in addition to the relative efficiency of the second cooling process. We determine the eigenvalues of the oscillation modes, and discuss the corresponding implications.

## 2 THE RADIATIVE ACCRETION SHOCK

The time-dependent mass continuity, momentum and energy equations for the planar post-shock accretion flow are

$$\frac{\partial \rho}{\partial t} + \rho \frac{\partial v}{\partial x} + v \frac{\partial \rho}{\partial x} = 0, \tag{1}$$

$$\rho \left( \frac{\partial v}{\partial t} + v \frac{\partial v}{\partial x} \right) + \frac{\partial P}{\partial x} = 0, \tag{2}$$

$$\frac{\partial P}{\partial t} + v \frac{\partial P}{\partial x} - \frac{5}{3} \frac{P}{\rho} \left( \frac{\partial \rho}{\partial t} + v \frac{\partial \rho}{\partial x} \right) = -\frac{2}{3} \Lambda_T, \tag{3}$$

where $P$, $v$ and $\rho$ are respectively the pressure, velocity and density of the stream, and $\Lambda_T$ is the composite radiative cooling function.

The cooling function is a composite of optically thin thermal bremsstrahlung plus another power-law cooling term:

$$\Lambda_T \equiv \Lambda_{\mathrm{br}} + \Lambda_2 = C \rho^2 \left( \frac{P}{\rho} \right)^{1/2} \left[ 1 + \epsilon_{\mathrm{s}} \left( \frac{P}{P_{\mathrm{s}}} \right)^{\alpha} \left( \frac{\rho}{\rho_{\mathrm{s}}} \right)^{-\beta} \right]. \tag{4}$$

These are expressed in terms of powers of density and pressure ($\alpha = b - 0.5$ and $\beta = 1.5 + b - a$). The constant $C = (2\pi k_{\mathrm{B}}/3m_{\mathrm{e}})^{1/2} (2^5 \pi e^6 / 3 h m_{\mathrm{e}} c^3)(\mu/k_{\mathrm{B}} m_{\mathrm{p}}^3)^{1/2} g_{\mathrm{B}}$, where $k_{\mathrm{B}}$ is the Boltzmann constant, $h$ the Planck constant, $c$ the speed of light, $e$ the electron charge, $m_{\mathrm{e}}$ the electron mass, $m_{\mathrm{p}}$ the proton mass, $\mu$ the mean molecular weight of the gas, and $g_{\mathrm{B}}$ the Gaunt factor (see Rybicki & Lightman 1979). The numerical value of $C$ is $3.9 \times 10^{16}$ in c.g.s. units, assuming that $\mu = 0.5$ and $g_{\mathrm{B}} = 1$. We assume the adiabatic index

$\gamma = 5/3$ for an ideal gas, and the equation of state is

$$P = \frac{\rho k_B T}{\mu m_H},\tag{5}$$

where $m_H$ is the mass of the a hydrogen atom. The efficiency of the second cooling process compared to the bremsstrahlung, evaluated at the shock, is given by $\epsilon_s$. For accretion on to white dwarfs in magnetic cataclysmic variables the second cooling mechanism is optically thick cyclotron cooling. An optically thick cooling process is generally not a simple energy-loss function. However, for typical parameters of accreting white dwarfs in magnetic cataclysmic variables, the cyclotron cooling can be mimicked by a power-law cooling function with indices $\alpha = 2.0$ and $\beta = 3.85$ (see Langer et al. 1982 and Saxton et al. 1997). In this approximation, the parameter $\epsilon_s$ increases monotonically with the white dwarf magnetic field.

We choose to express the composite cooling function in terms of the bremsstrahlung cooling, so that the second cooling function goes to zero as the density becomes infinite. This allows us to use the same boundary conditions at the dwarf surface in all cases, so that we may have confidence that stability effects will be due only to the properties of the cooling functions, and not the boundary conditions at the white dwarf surface. Alternatively, the temperature could have been made to go to a finite value at the white dwarf surface, but this approach is mathematically equivalent, except that the new boundary conditions are less obvious, especially for the perturbed variables.

## 3   PERTURBATION ANALYSIS

We consider a first-order perturbation of the steady-state solution for the post-shock gas flow, with the shock height and the pressure, density and velocity fields expressed as:

$$x_s = x_{s0} + x_{s1}e^{\omega t},\tag{6}$$

$$P(\xi, t) = P_0(\xi) + P_1(\xi)e^{\omega t},\tag{7}$$

$$\rho(\xi, t) = \rho_0(\xi) + \rho_1(\xi)e^{\omega t},\tag{8}$$

$$v(\xi, t) = v_0(\xi) + v_1(\xi)e^{\omega t},\tag{9}$$

where $\xi = x/x_s$ is a dimensionless altitude coordinate, and $\omega = v_{s1}/x_{s1}$ is a frequency scale of the perturbations. The subscripts '0' and '1' denote steady-state variables and first-order perturbation respectively; 's' denotes variables evaluated at the shock surface.

We consider expressions in terms of the dimensionless steady-state velocity ($\tau \equiv -v_0/v_{ff}$) to simplify the form of the equations. The steady-state solution is completely described by a differential equation for its velocity profile:

$$\xi'(\tau) \equiv \frac{d\xi}{d\tau} = \frac{1}{1 + \epsilon_s f(\tau)} \frac{\tau^2(5 - 8\tau)}{\sqrt{\tau(1 - \tau)}},\tag{10}$$

where

$$f(\tau) = \frac{4^{\alpha+\beta}}{3^\alpha}(1 - \tau)^\alpha \tau^\beta\tag{11}$$

(see Wu 1994). For the case of bremsstrahlung cooling alone ($\epsilon_s = 0$) there exists an analytic solution (Aizu 1973), but for the general two-process cooling function it is necessary to carry out a numerical integration of the closed-form solution.

It is convenient to define further dimensionless complex variables to describe the perturbed solutions: $\zeta = x_{s0}\omega\rho_1/v_{s1}\rho_a$, $\pi = P_1/\rho_a v_{ff}v_{s1}$, $\eta = v_1/v_{s1}$ and $\delta = x_{s0}\omega/v_{ff}$. The first three relate to perturbed density, pressure and velocity. The last serves as a dimensionless eigenfrequency, $\delta = \delta_R + i\delta_I$, where $\delta_I$ is the oscillatory part, and $\delta_R$ is a growth/decay term. Then the mass continuity, momentum and energy equations give rise to three coupled complex linear differential equations in the perturbed variables:

$$-\zeta\frac{d\xi}{d\tau} + \frac{\tau}{\delta}\frac{d\zeta}{d\tau} - \frac{1}{\tau}\frac{d\eta}{d\tau} - \frac{\xi}{\tau^2} + \frac{\zeta}{\delta} + \frac{\eta}{\tau^2} = 0,\tag{12}$$

$$-\delta\eta\frac{d\xi}{d\tau} + \tau\frac{d\eta}{d\tau} - \tau\frac{d\pi}{d\tau} - \xi + \eta - \frac{\zeta\tau^2}{\delta} = 0,\tag{13}$$

$$-\pi\delta\frac{d\xi}{d\tau} - \frac{5}{3}(1 - \tau)\frac{d\eta}{d\tau} + \tau\frac{d\pi}{d\tau} - \xi + \eta + \frac{5}{3}\pi = \frac{(5 - 8\tau)}{3}\left[\frac{1}{\delta} + \frac{f_1(\tau)\pi}{2(1 - \tau)} + \frac{3}{2}f_2(\tau)\frac{\tau\zeta}{\delta}\right],\tag{14}$$

where the functions $f_1(\tau)$ and $f_2(\tau)$ are defined as:

$$f_1(\tau) = 1 + \frac{2\epsilon_s\alpha f(\tau)}{1 + \epsilon_s f(\tau)},\tag{15}$$

$$f_2(\tau) = 1 - \frac{2}{3}\left[\frac{\epsilon_s\beta f(\tau)}{1 + \epsilon_s f(\tau)}\right],\tag{16}$$

and $f(\tau)$ is defined in equation (11).

Equations (12), (13) and (14) are solved for $d\zeta/d\tau$, $d\eta/d\tau$ and $d\pi/d\tau$. The resulting differential equations are split into real and imaginary

parts to yield six first-order differential equations in the real variables $\delta_R$, $\delta_I$, $\zeta_R$, $\zeta_I$, $\eta_R$, $\eta_I$, $\pi_R$ and $\pi_I$, and the known variables of the static solution, $\alpha$, $\beta$ and $\xi(\tau)$:

$$\frac{d\zeta_R}{d\tau} = \left[\left(\frac{5-14\tau}{5-8\tau}\right)\frac{\xi(\tau)}{\tau^3}\delta_R - \frac{1}{\tau^2}\right] - \frac{1}{\tau}\left[(2-\alpha)f_2(\tau) + 5\left(\frac{1-\tau}{5-8\tau}\right) - \xi'(\tau)\delta_R\right]\zeta_R - \left[\frac{\xi'(\tau)}{\tau}\delta_I\right]\zeta_I$$
$$- \left[\left(\frac{5-14\tau}{5-8\tau}\right)\frac{1}{\tau^3}\delta_R + \left(\frac{3\xi'(\tau)}{\tau^2(5-8\tau)}\right)(\delta_R^2 - \delta_I^2)\right]\eta_R - \left[\left(\frac{5-14\tau}{5-8\tau}\right)\frac{1}{-\tau^3}\delta_I - \left(\frac{6\xi'(\tau)}{\tau^2(5-8\tau)}\right)\delta_R\delta_I\right]\eta_I$$
$$- \left[\left(\frac{\alpha f_1(\tau)}{1-\tau} - \frac{5}{5-8\tau}\right)\delta_R + \frac{3\xi'(\tau)(\delta_R^2 - \delta_I^2)}{5-8\tau}\right]\frac{\pi_R}{\tau^2} + \left[\left(\frac{\alpha f_1(\tau)}{1-\tau} - \frac{5}{5-8\tau}\right)\delta_I + \frac{6\xi'(\tau)\delta_R\delta_I}{5-8\tau}\right]\frac{\pi_I}{\tau^2}, \tag{17}$$

$$\frac{d\zeta_I}{d\tau} = \left[\left(\frac{5-14\tau}{5-8\tau}\right)\frac{\xi(\tau)}{\tau^3}\delta_I\right] + \left[\frac{\xi'(\tau)}{\tau}\delta_I\right]\zeta_R - \frac{1}{\tau}\left[(2-\alpha)f_2(\tau) + 5\left(\frac{1-\tau}{5-8\tau}\right) - \xi'(\tau)\delta_R\right]\zeta_I - \left[\left(\frac{5-14\tau}{5-8\tau}\right)\frac{1}{\tau^3}\delta_I + \left(\frac{6\xi'(\tau)}{\tau^2(5-8\tau)}\right)\delta_R\delta_I\right]\eta_R$$
$$- \left[\left(\frac{5-14\tau}{5-8\tau}\right)\frac{1}{\tau^3}\delta_R + \left(\frac{3\xi'(\tau)}{\tau^2(5-8\tau)}\right)(\delta_R^2 - \delta_I^2)\right]\eta_I - \left[\left(\frac{\alpha f_1(\tau)}{1-\tau} - \frac{5}{5-8\tau}\right)\delta_I + \frac{6\xi'(\tau)\delta_R\delta_I}{5-8\tau}\right]\frac{\pi_R}{\tau^2}$$
$$- \left[\left(\frac{\alpha f_1(\tau)}{1-\tau} - \frac{5}{5-8\tau}\right)\delta_R + \frac{3\xi'(\tau)(\delta_R^2 - \delta_I^2)}{5-8\tau}\right]\frac{\pi_I}{\tau^2}, \tag{18}$$

$$\frac{d\eta_R}{d\tau} = -\left[\frac{6\xi(\tau)}{5-8\tau} + \frac{\delta_R}{\delta_R^2 + \delta_I^2}\right] - \left[\frac{3\tau^2}{5-8\tau} + (2-\alpha)\tau f_2(\tau)\right]\frac{\delta_R}{\delta_R^2 + \delta_I^2}\zeta_R - \left[\frac{3\tau^2}{5-8\tau} + (2-\alpha)\tau f_2(\tau)\right]\frac{\delta_I}{\delta_R^2 + \delta_I^2}\zeta_I$$
$$+ \left[\frac{3}{5-8\tau}(2 - \xi'(\tau)\delta_R)\right]\eta_R + \left[\frac{3}{5-8\tau}\xi'(\tau)\delta_I\right]\eta_I - \left[\frac{\alpha f_1(\tau)}{1-\tau} + \frac{3\xi'(\tau)\delta_R - 5}{5-8\tau}\right]\pi_R + \left[\frac{3}{5-8\tau}\xi'(\tau)\delta_I\right]\pi_I, \tag{19}$$

$$\frac{d\eta_I}{d\tau} = +\left[\frac{\delta_I}{\delta_R^2 + \delta_I^2}\right] + \left[\frac{3\tau^2}{5-8\tau} + (2-\alpha)\tau f_2(\tau)\right]\frac{\delta_I}{\delta_R^2 + \delta_I^2}\zeta_R - \left[\frac{3\tau^2}{5-8\tau} + (2-\alpha)\tau f_2(\tau)\right]\frac{\delta_R}{\delta_R^2 + \delta_I^2}\zeta_I$$
$$- \left[\frac{3}{5-8\tau}\xi'(\tau)\delta_I\right]\eta_R + \left[\frac{3}{5-8\tau}(2 - \xi'(\tau)\delta_R)\right]\eta_I - \left[\frac{3}{5-8\tau}\xi'(\tau)\delta_I\right]\pi_R - \left[\frac{\alpha f_1(\tau)}{1-\tau} + \frac{3\xi'(\tau)\delta_R - 5}{5-8\tau}\right]\pi_I, \tag{20}$$

$$\frac{d\pi_R}{d\tau} = -\left[\left(\frac{\delta_R}{\delta_R^2 + \delta_I^2}\right) - \left[\frac{5-2\tau}{-\tau(5-8\tau)}\right]\xi(\tau)\right] - \left[(2-\alpha)\tau f_2(\tau) - \left(\frac{5\tau(\tau-1)}{5-8\tau}\right)\right]\frac{\delta_R}{\delta_R^2 + \delta_I^2}\zeta_R$$
$$- \left[(2-\alpha)\tau f_2(\tau) - \left(\frac{5\tau(\tau-1)}{5-8\tau}\right)\right]\frac{\delta_I}{\delta_R^2 + \delta_I^2}\zeta_I + \left[\frac{5-2\tau}{\tau} - 5\left(\frac{1-\tau}{\tau}\right)\xi'(\tau)\delta_R\right]\frac{1}{5-8\tau}\eta_R + \left[5\left(\frac{1-\tau}{\tau}\right)\xi'(\tau)\delta_I\right]\frac{1}{5-8\tau}\eta_I$$
$$- \left[\frac{\alpha f_1(\tau)}{1-\tau} + \frac{3\xi'(\tau)\delta_R - 5}{5-8\tau}\right]\pi_R + \left[\frac{3}{5-8\tau}\xi'(\tau)\delta_I\right]\pi_I, \tag{21}$$

$$\frac{d\pi_I}{d\tau} = +\left[\frac{\delta_I}{\delta_R^2 + \delta_I^2}\right] + \left[(2-\alpha)\tau f_2(\tau) - \left(\frac{5\tau(\tau-1)}{5-8\tau}\right)\right]\frac{\delta_I}{\delta_R^2 + \delta_I^2}\zeta_R - \left[(2-\alpha)\tau f_2(\tau) - \left(\frac{5\tau(\tau-1)}{5-8\tau}\right)\right]\frac{\delta_R}{\delta_R^2 + \delta_I^2}\zeta_I$$
$$- \left[5\left(\frac{1-\tau}{\tau}\right)\xi'(\tau)\delta_I\right]\frac{1}{5-8\tau}\eta_R + \left[\frac{5-2\tau}{\tau} - 5\left(\frac{1-\tau}{\tau}\right)\xi'(\tau)\delta_R\right]\frac{1}{5-8\tau}\eta_I - \left[\frac{3}{5-8\tau}\xi'(\tau)\delta_I\right]\pi_R - \left[\frac{\alpha f_1(\tau)}{1-\tau} + \frac{3\xi'(\tau)\delta_R - 5}{5-8\tau}\right]\pi_I. \tag{22}$$

## 4 RESULTS

### 4.1 Eigenmodes

The six differential equations (17)–(22) are integrated numerically using a Runge–Kutta method with appropriate boundary conditions. In terms of the dimensionless perturbed variables, the conditions at the shock ($\tau = 1/4$) are $\zeta_R = 0$, $\zeta_I = 0$, $\eta_R = 3/4$, $\eta_I = 0$, $\pi_R = 3/2$ and $\pi_I = 0$. At the dwarf surface ($\tau = 0$) there are no specific conditions on the values of $\zeta_R$, $\zeta_I$, $\pi_R$ and $\pi_I$, but the stationary wall condition ($\eta_R = 0$, $\eta_I = 0$) applies (see Chevalier & Imamura 1982 and Saxton et al. 1997). Integration proceeds between $\tau = 0$ and $\tau = 1/4$ for trial values of $\delta_R$ and $\delta_I$. Values of the $\delta$s are sought which yield $\eta_R = \eta_I = 0$ at $\tau = 0$ (see Appendix A). Each of these eigenvalues corresponds to an oscillatory mode of the shock. The modes form a sequence consisting of a fundamental mode and a succession of overtones.

We investigated cases with 13 different choices of $(\alpha, \beta)$, and $\epsilon_s$ took values of 0.1, $10^{-2/3}$, $10^{-1/3}$, 1, $10^{1/3}$, $10^{2/3}$ and 10. The first set are systems with $\Lambda_2 \propto \rho^{0.15}T^{2.5}$, $\alpha = 2.0$ and $\beta = 3.85$. This is appropriate for accreting white dwarfs in magnetic cataclysmic variables, in which bremsstrahlung and cyclotron cooling are important (see Wu, Chanmugam & Shaviv 1994). We are aware that the cyclotron cooling in these systems is, in fact, optically thick. For an exact treatment one needs to consider the coupled time-dependent hydrodynamic and radiative transfer equations. However, to make the problem tractable in this linear analysis, we assume a simple power-law cooling approximation. The results are shown in Table 1.

**Table 1.** Eigenvalues for the first eight modes of systems with bremsstrahlung plus cyclotron cooling, for various values of the cyclotron cooling efficiency at shock ($\epsilon_s$), expressed as $\delta_R$ and $\delta_I$.

| $\epsilon_s = 0$ | | $\log \epsilon_s = -1$ | | $\log \epsilon_s = -2/3$ | |
|---|---|---|---|---|---|
| −0.010 | 0.305 | −0.017 | 0.308 | −0.025 | 0.311 |
| 0.047 | 0.887 | 0.040 | 0.881 | 0.032 | 0.874 |
| 0.061 | 1.504 | 0.053 | 1.493 | 0.044 | 1.481 |
| 0.085 | 2.107 | 0.078 | 2.090 | 0.070 | 2.072 |
| 0.088 | 2.723 | 0.080 | 2.701 | 0.071 | 2.677 |
| 0.107 | 3.331 | 0.098 | 3.306 | 0.090 | 3.275 |
| 0.104 | 3.944 | 0.096 | 3.911 | 0.087 | 3.876 |
| 0.121 | 4.555 | 0.113 | 4.517 | 0.104 | 4.478 |

| $\log \epsilon_s = -1/3$ | | $\log \epsilon_s = 0$ | | $\log \epsilon_s = 1/3$ | |
|---|---|---|---|---|---|
| −0.039 | 0.316 | −0.061 | 0.322 | −0.092 | 0.325 |
| 0.018 | 0.861 | −0.036 | 0.838 | −0.030 | 0.803 |
| 0.029 | 1.458 | 0.003 | 1.419 | −0.033 | 1.357 |
| 0.055 | 2.037 | 0.033 | 1.978 | 0.004 | 1.887 |
| 0.055 | 2.632 | 0.028 | 2.553 | −0.008 | 2.429 |
| 0.075 | 3.219 | 0.051 | 3.124 | 0.019 | 2.978 |
| 0.071 | 3.808 | 0.046 | 3.691 | 0.012 | 3.510 |
| 0.088 | 4.402 | 0.063 | 4.270 | 0.025 | 4.068 |

| $\log \epsilon_s = 2/3$ | | $\log \epsilon_s = 1$ | |
|---|---|---|---|
| −0.126 | 0.322 | −0.156 | 0.309 |
| −0.057 | 0.758 | −0.077 | 0.707 |
| −0.077 | 1.271 | −0.119 | 1.161 |
| −0.029 | 1.771 | −0.065 | 1.637 |
| −0.047 | 2.267 | −0.077 | 2.057 |
| −0.023 | 2.786 | −0.073 | 2.553 |
| −0.021 | 3.267 | −0.045 | 2.986 |
| −0.021 | 3.794 | −0.069 | 3.456 |

The other 12 choices of $(\alpha, \beta)$ represent second cooling processes which are like cyclotron cooling in so far as they tend to stabilize the shock against oscillations, competing with the effect of bremsstrahlung. The first four choices of cooling mechanisms are first-order in density ($\Lambda_2 \propto \rho T^b$, $\beta = \alpha + 1$); next four choices are of the form $\Lambda_2 \propto \rho^{1.5} T^b$ ($\beta = \alpha + 0.5$); the last four choices are second-order in density ($\Lambda_2 \propto \rho^2 T^b$, $\beta = \alpha$).

For each case we investigate the stability of harmonics under conditions with bremsstrahlung dominant over ($\epsilon_s = 0.1, 10^{-2/3}, 10^{-1/3}$), comparable to ($\epsilon_s = 1$), or dominated by the second cooling mechanism ($\epsilon_s = 10^{1/3}, 10^{2/3}, 10$) at the shock surface. The choice of $\epsilon_s = 0$ corresponds to the special restricted case of the bremsstrahlung-only shock. Applying this limit to our equations exactly recovers earlier results (e.g. Chevalier & Imamura 1982) for the single-cooling, bremsstrahlung-only case.

## 4.2 Frequencies

In all cases the oscillatory part of the eigenvalue is found to be quantized like the modal frequencies of a pipe open at one end. This can be expressed as a linear fit, $\delta_I = (n - 1/2)\delta_{IO} + \delta_C$, where $n$ is the harmonic number, $\delta_{IO}$ is a frequency spacing and $\delta_C$ is a small offset correction. These constants depend upon the indices $(\alpha, \beta)$ and efficiency ($\epsilon_s$) of the second cooling process. (See Appendix B for values of these constants derived from fits to the first eight modes of each system.)

For a purely bremsstrahlung-dominated shock $\delta_{IO} \approx 0.609$, but the mode spacing becomes significantly smaller as the second cooling process increases in importance. For a given stabilizing cooling mechanism $(\alpha, \beta)$, the mode spacing decreases monotonically as $\epsilon_s$ increases. The variation of $\delta_{IO}$ with $\epsilon_s$ is almost identical for all cases other than those with $\alpha = 0.5$ and $\beta < \alpha + 1$. In these exceptional cases, the mode spacing decreases much more slowly with increasing $\epsilon_s$. The special characteristic of these systems is that the second cooling function's temperature dependence is weaker than the density dependence (i.e., $\Lambda_2 \propto \rho^a T^b$, with $b < a$).

For most sets of cooling indices, the frequency offset, $\delta_C$, increases steadily with $\epsilon_s$, in the range studied. This is the case for bremsstrahlung plus cyclotron cooling. Except for the $\beta = \alpha$ systems, the rise of $\delta_C$ with $\epsilon_s$ is consistently steeper for lower $\alpha$. In some high-$\alpha$ cases with $\beta = \alpha$ and $\beta = \alpha + 0.5$, $\delta_C$ decreases after reaching a maximum at some $\epsilon_s$. The peak occurs at lower $\epsilon_s$ when $\alpha$ is greater.

## 4.3 Stability properties

Stability of a particular mode is indicated by the sign of the growth/decay term $\delta_R$. Positive values indicate instability; negative values indicate stability.

The most unstable system investigated is that with bremsstrahlung cooling only. In this case the first unstable mode is the second harmonic. Because the fundamental is stable even when bremsstrahlung cooling is the only mechanism, cases including a stabilizing cooling process become unstable at the second or higher harmonic.

Systems with a particular density dependence in the second cooling mechanism $\Lambda_2 \propto \rho^a T^b$ share the same value of $a = 2 + \alpha - \beta$. If these cases are considered together, those in which $\Lambda_2$ depends on a higher power of temperature ($b = \alpha + 0.5$) have modes which are more stable for a given value of $\epsilon_s$.

For given $(\alpha, \beta)$ and $\epsilon_s$ there is a general trend towards greater instability with increasing harmonic number. This can be seen in any of the curves of Figs 1, 2 and 3. Modes of lower harmonic number tend to be stable, and higher modes either less stable or else genuinely unstable.
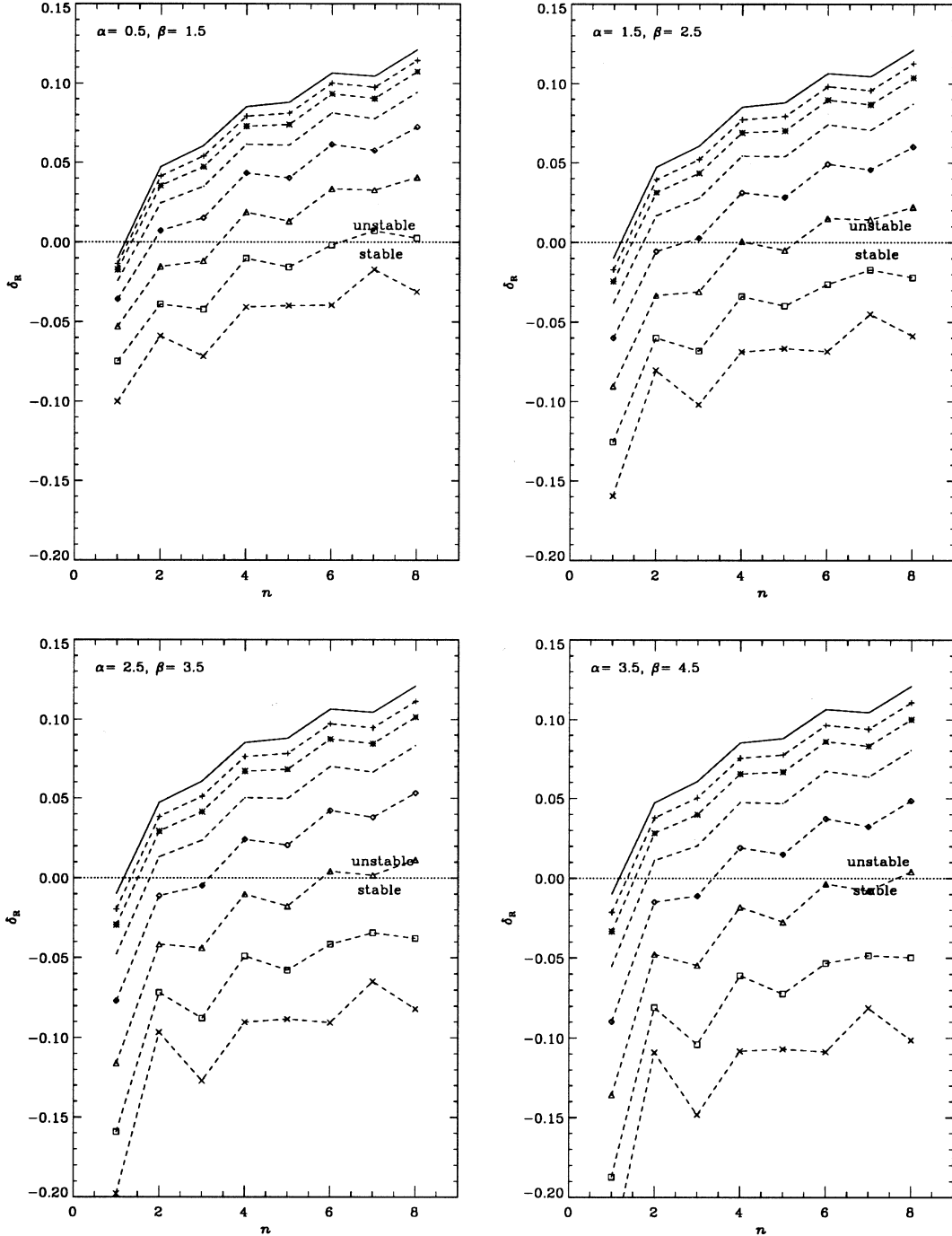


**Figure 1.** The real part of the eigenvalues, $\delta_R$, as a function of the harmonic number $n$, for cooling power-law indices $\alpha = 0.5, 1.5, 2.5$ and $3.5$, and $\beta = \alpha + 1$. Solid lines refer to the stability of the bremsstrahlung-only case. From top to bottom, the dashed lines correspond to systems with different values of the cooling efficiency, with $\epsilon_s = 0.1, 10^{-2/3}, 10^{-1/3}, 1, 10^{1/3}, 10^{2/3}$ and $10$.

This trend of modal instability rises sharply between successive modes with low $n$, and slowly for higher harmonic number. The number of modes we have considered is insufficient to determine their asymptotic behaviour as $n \to \infty$.

If we consider the stability of the sequence of modes for a particular case of $(\alpha, \beta)$, increasing the efficiency of the second cooling mechanism ($\epsilon_s$) stabilizes more of the lower modes. The indices of the second cooling process $(\alpha, \beta)$ determine how rapidly the modes cross from instability to stability as $\epsilon_s$ increases.

However, the detailed behaviour of the $\delta_R$ sequence with respect to $n$ is not strictly monotonic. On top of the general trend to increasing stability consecutive modes deviate towards greater or lesser stability. For low $\epsilon_s$ these deviations follow an odd–even step pattern similar to that shown by the bremsstrahlung-only modes. For higher $\epsilon_s$ the deviations are of greater magnitude and follow a more complicated sequence. The cooling indices $(\alpha, \beta)$ determine the form of this sequence in the limit of high $\epsilon_s$.
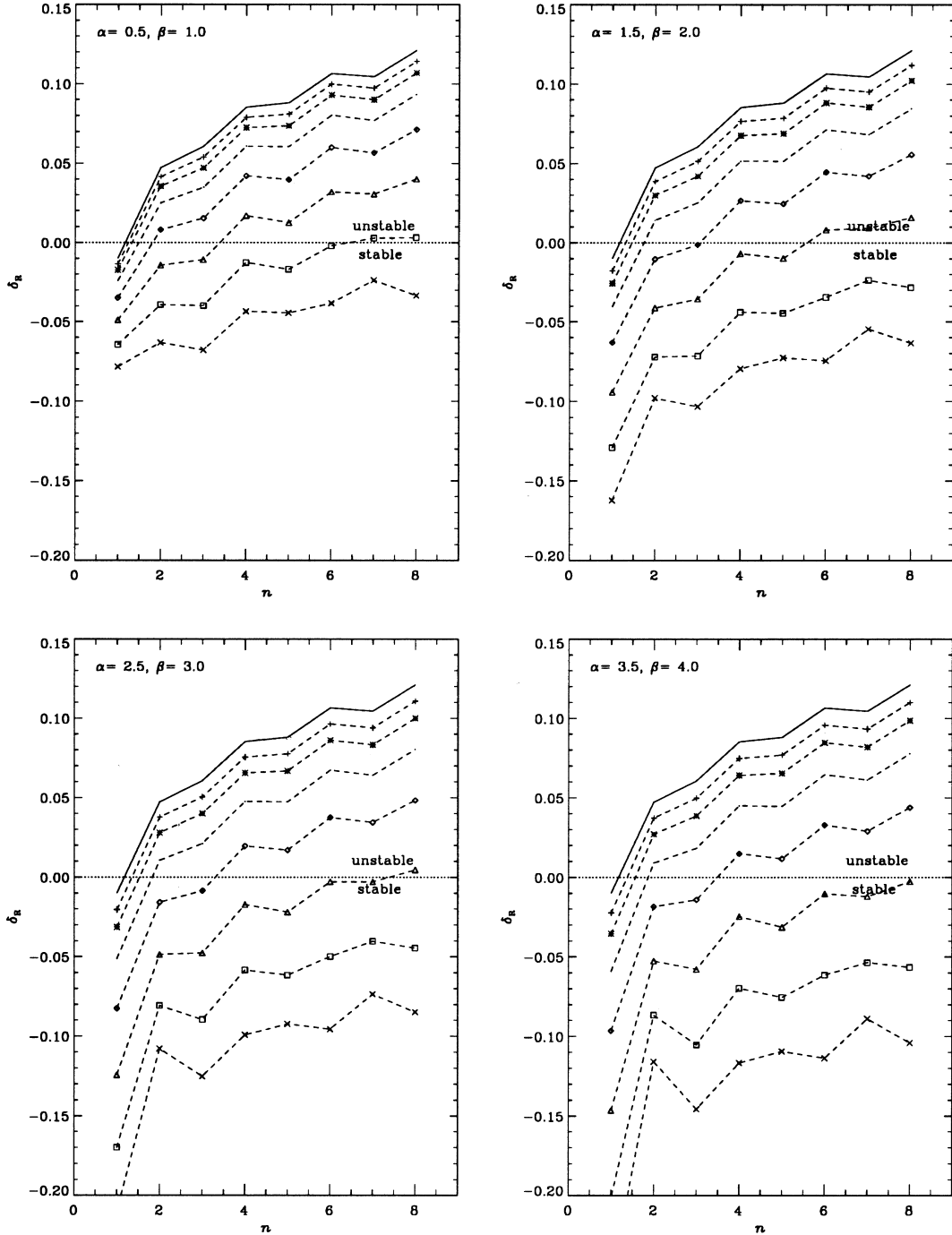


**Figure 2.** The real part of the eigenvalues, $\delta_R$, as a function of the harmonic number $n$, for cooling power-law indices $\alpha = 0.5, 1.5, 2.5$ and $3.5$, and $\beta = \alpha + 0.5$. Solid lines refer to the stability of the bremsstrahlung-only case. From top to bottom, the dashed lines correspond to systems with different values of the cooling efficiency, with $\epsilon_s = 0.1, 10^{-2/3}, 10^{-1/3}, 1, 10^{1/3}, 10^{2/3}$ and $10$.

These growing deviations often result in a mode $n$ being marginally unstable, but a higher mode $n + 1$ being stable. This is important when considering which mode is the lowest unstable mode $n_* = n_*(\epsilon_s)$. As $\epsilon_s$ increases, it passes through critical values where what was formerly the least unstable mode becomes stable, and a higher mode is the new $n_*$. If at some $\epsilon_s$ there is a mode $n > n_*$ which is already stable, then there will never be a value of $\epsilon_s$ that makes $n$ become the new $n_*$. For given $(\alpha, \beta)$ there are certain modes that can never be the first unstable mode for any value of $\epsilon_s$. For the 13 different choices of $(\alpha, \beta)$ studied, Table 2 records which harmonic was the lowest unstable mode at different $\epsilon_s$.

For a given mode, stability only ever increases with increasing $\epsilon_s$, regardless of the behaviour of the overall pattern. The deviations of the stability curve reflect only a tendency for some particular modes to stabilize faster or sooner than others. They never grow enough to raise low
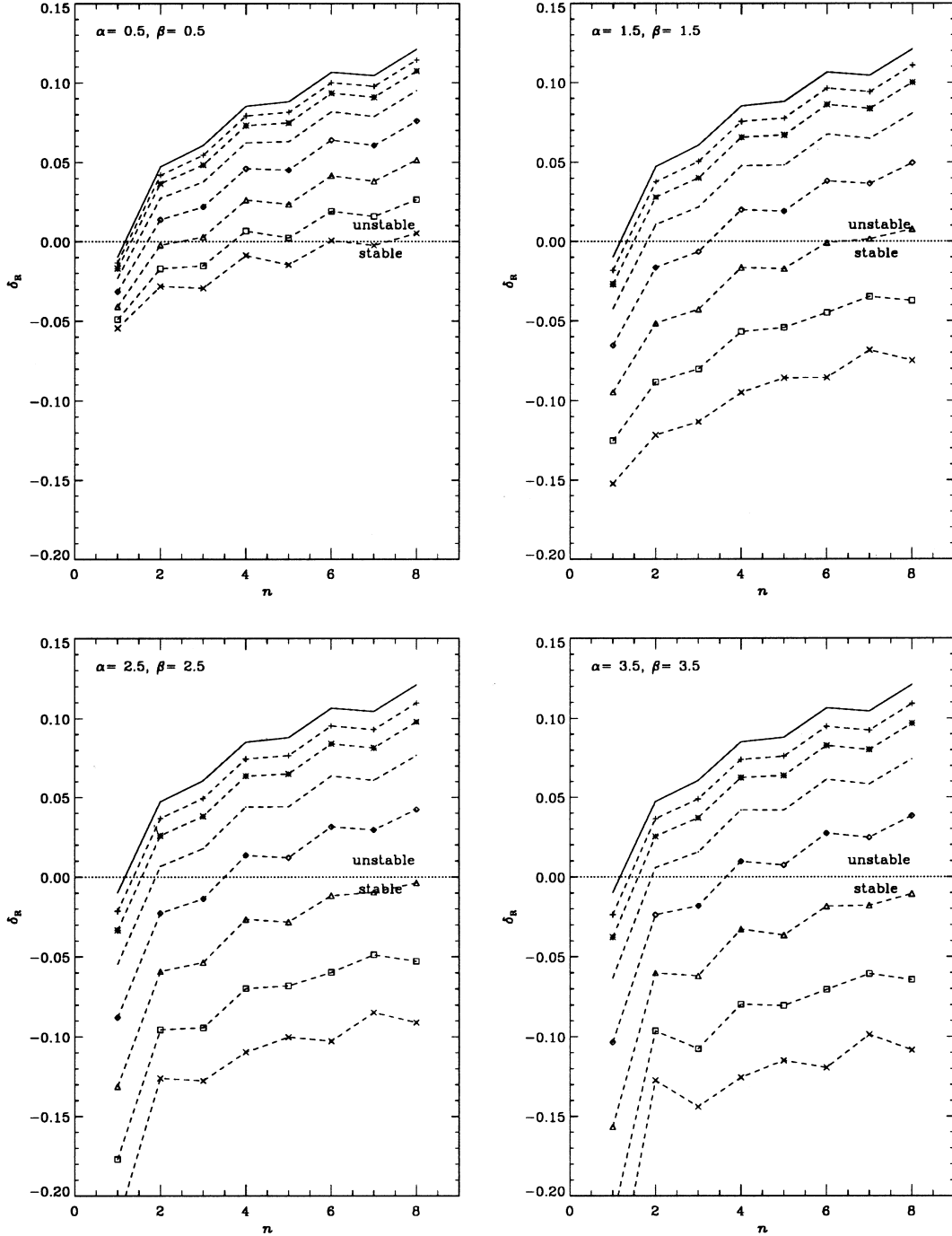


**Figure 3.** The real part of the eigenvalues, $\delta_R$, as a function of the harmonic number $n$, for cooling power-law indices $\alpha = 0.5, 1.5, 2.5$ and $3.5$, and $\beta = \alpha$. Solid lines refer to the stability of the bremsstrahlung-only case. From top to bottom, the dashed lines correspond to systems with different values of the cooling efficiency, with $\epsilon_s = 0.1, 10^{-2/3}, 10^{-1/3}, 1, 10^{1/3}, 10^{2/3}$ and $10$.

**Table 2.** First unstable mode $n_*$ for systems with various values of the power-law indices and the efficiency of the second cooling process. The first case listed is that of bremsstrahlung plus cyclotron cooling. The next four are the $\Lambda_2 \propto \rho T^b$ systems; the following four are $\Lambda_2 \propto \rho^{1.5} T^b$ systems; and the last four are the $\Lambda_2 \propto \rho^2 T^b$ systems.

| $(\alpha, \beta)$ | | $\log \epsilon_s$ | | | | | | |
|---|---|---|---|---|---|---|---|---|
| | | $-1$ | $-\frac{2}{3}$ | $-\frac{1}{3}$ | $0$ | $+\frac{1}{3}$ | $+\frac{2}{3}$ | $+1$ |
| 2.0 | 3.85 | 2 | 2 | 2 | 3 | 4 | – | – |
| 0.5 | 1.5 | 2 | 2 | 2 | 2 | 4 | 7 | – |
| 1.5 | 2.5 | 2 | 2 | 2 | 3 | 4 | – | – |
| 2.5 | 3.5 | 2 | 2 | 2 | 4 | 6 | – | – |
| 3.5 | 4.5 | 2 | 2 | 2 | 4 | 8 | – | – |
| 0.5 | 1.0 | 2 | 2 | 2 | 2 | 4 | 7 | – |
| 1.5 | 2.0 | 2 | 2 | 2 | 4 | 6 | – | – |
| 2.5 | 3.0 | 2 | 2 | 2 | 4 | 8 | – | – |
| 3.5 | 4.0 | 2 | 2 | 2 | 4 | – | – | – |
| 0.5 | 0.5 | 2 | 2 | 2 | 2 | 3 | 4 | 6 |
| 1.5 | 1.5 | 2 | 2 | 2 | 4 | 7 | – | – |
| 2.5 | 2.5 | 2 | 2 | 2 | 4 | – | – | – |
| 3.5 | 3.5 | 2 | 2 | 2 | 4 | – | – | – |

modes back into the regime of instability, and they always grow more slowly than the dropping of the trend curve into the stable regime of the eigenplane.

Comparing the time-scale of the second cooling process, $t_2$, with the oscillation time-scales the modes, $t_{osc} = (x_{s0}/v_{ff})2\pi\delta_I/(\delta_R^2 + \delta_I^2)$, reveals a regularity in the modes' stability properties. Every mode with oscillatory time-scale $t_{osc} > t_2$ is a stable mode, as shown in the case of bremsstrahlung plus cyclotron cooling (see Figs 4, 5 and 6), and in all other cases studied (not shown) except for $\alpha = \beta = 0.5$ and $\epsilon_s = 1$. The converse is not generally true: modes with $t_{osc} < t_2$ are not always unstable. Modes with $t_{osc} < t_2$ are more often stable if $t_{osc}$ is close to $t_2$, but there is no strict rule.

## 5   DISCUSSION

Our work recovers the earlier results of Chevalier & Imamura (1982) for the limit of purely bremsstrahlung cooling, which shows that the fundamental mode is stable and the overtones unstable. Earlier works (e.g. Chevalier & Imamura 1982; Bertschinger 1986; Houck & Chevalier 1992; Tóth & Draine 1993; Dgani & Soker 1994) represented systems with multiple cooling processes via a single power law with intermediate indices. However, the validity of this approach is unclear in cases when an additional cooling process is important (e.g., cyclotron cooling in the accretion on to a strongly magnetic white dwarf). A cooling process with a destabilizing tendency and a cooling process with a stabilizing tendency may alternately dominate over different parts of the oscillatory cycle. This competition of effects warrants explicit treatment. We extend and replace the conventional single-cooling formulation with the more physically realistic case where two power-law cooling terms are explicitly summed, one with a destabilizing influence and the other tending to suppress oscillations.

Our work does not include two-temperature effects (like those of Imamura et al. 1996). The analysis is therefore inapplicable in systems where the radiative cooling time-scale is much shorter than the electron–ion energy exchange time-scale.

The particular systems we study – shocks in white dwarfs in magnetic cataclysmic variables – are not geometrically extended in the direction of the accretion flow (see, e.g., Cropper 1990), so non-planar perturbations (Bertschinger 1986; Imamura et al. 1996) and transverse post-shock mass-loss (Dgani & Soker 1994) are unimportant. The shock sits above the white dwarf surface within a height that is only a small fraction of the white dwarf's radius, so the effects of the altitude variations of the gravity field (investigated by Houck & Chevalier 1992) can be neglected.

Stabilization of modes proceeds monotonically as the efficiency of the stabilizing cooling process ($\epsilon_s$) increases, although some modes stabilize more quickly than others. For a given $\epsilon_s$ higher harmonics are generally less stable, but between successive modes there are significant deviations from the trend. For low cooling efficiency (low $\epsilon_s$) these stability deviations follow an odd–even pattern. In the limit of high $\epsilon_s$, the pattern of deviations is less simple and depends on the power-law indices $(\alpha, \beta)$ of the second cooling function. The deviations become larger as $\epsilon_s$ increases, with the most stable modes stabilizing more effectively for a certain change in $\epsilon_s$.

A consequence of these deviations is that while a particular mode is marginally unstable, the next higher mode may sometimes be stable. Therefore the progression of the lowest unstable mode with increasing $\epsilon_s$ may jump from one harmonic to a higher harmonic, skipping one or more intermediate modes. This behavioural detail is not revealed in earlier analytic studies, which failed to consider whether or not instability of a mode $n$ automatically implies the instability of all higher modes.

It has been suggested that the oscillation time-scale of the radiative shock is approximately equal to the effective cooling time-scale of the post-shock matter (see, e.g., Langer et al. 1981). While this may be valid for shocks with a simple cooling law, it is not justified when two competing cooling processes are present. As shown in Figs 4, 5 and 6, the cyclotron and bremsstrahlung cooling time-scales are very different for different $\epsilon_s$, but the oscillation time-scale of each eigenmode does not change significantly. The effective cooling time-scale, which is

**Figure 6.** Same as Fig. 4 for $\epsilon_s = 10$.

**Figure 5.** Same as Fig. 4 for $\epsilon_s = 1$.
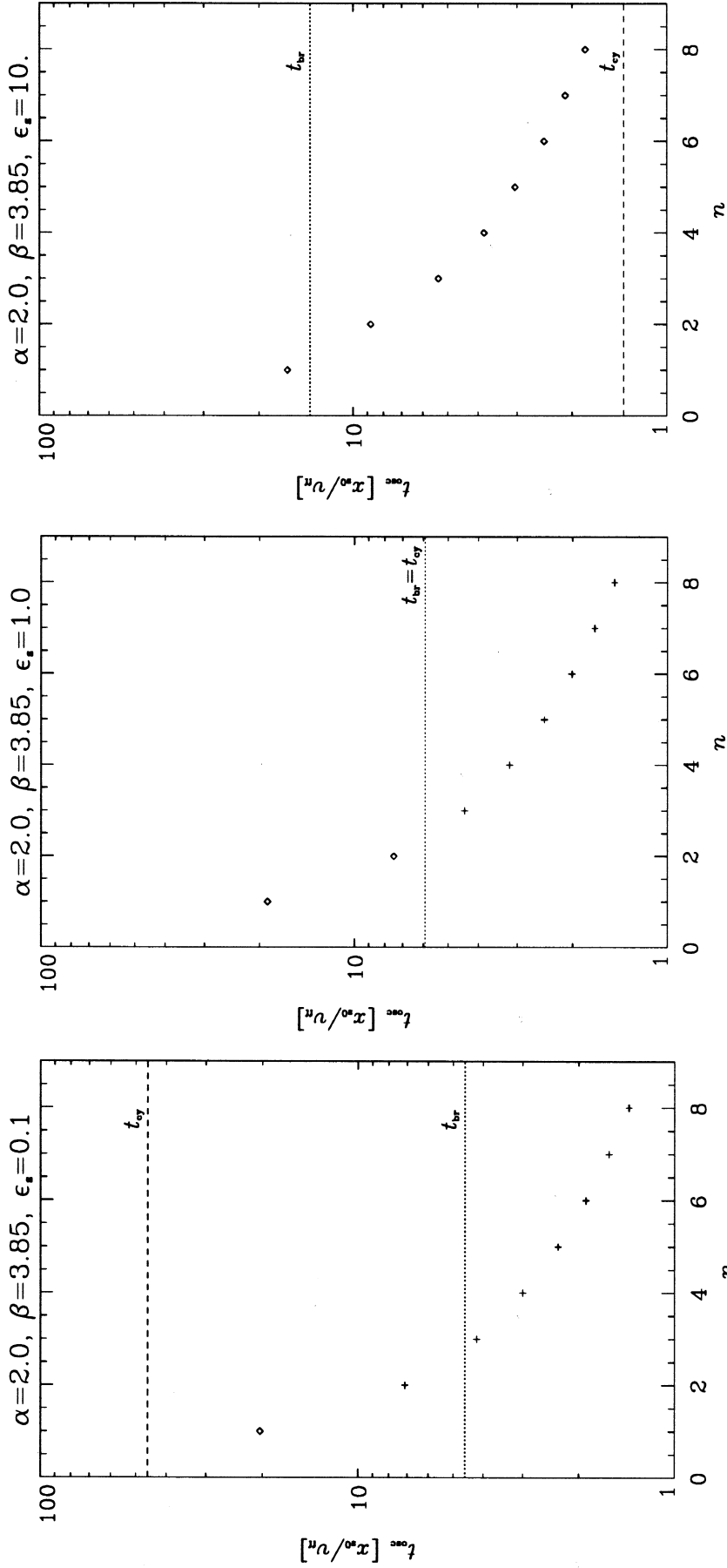
**Figure 4.** Oscillation time-scales of the first eight eigenmodes of the $\epsilon_s = 0.1$ bremsstrahlung plus cyclotron system, in units of $x_{s0}/v_{\text{ff}1}$, compared with the cooling time-scales for bremsstrahlung (dotted line) and cyclotron (dashed line). Stable modes are marked with diamonds ($\Diamond$); unstable modes are marked with crosses ($+$).

approximately the smaller one of the bremsstrahlung and cyclotron cooling time-scales, do not show strong association with the oscillation time-scale of any of the stable or unstable eigenmodes. The modes are, however, stable if their oscillation time-scales are larger than the cooling time-scale of the process with stabilizing effects.

Finally, we note that the analysis presented here proves only the instability in certain modes. It is unable to verify if a system is truly stable, since the system in principle has infinite modes, and we cannot survey all the modes in practice.

## 6  CONCLUSIONS

We examined the stability properties of the first eight modes of single-fluid, one-dimensional, radiative shocks with boundary conditions suitable for accretion on to a solid surface. A composite cooling function was used, explicitly summing contributions from thermal bremsstrahlung (which tends to destabilize the shock) and one of a variety of cooling processes chosen for a stabilizing effect. Some of these cases correspond to the situation of the stand-off shock in the accretion flow on to a magnetic white dwarf, with bremsstrahlung plus cyclotron cooling and the post-shock region standing close to the dwarf surface. Four of the mechanisms chosen are first-order in density ($\Lambda_2 \propto \rho T^b$), four are of order 3/2 in density ($\Lambda_2 \propto \rho^{1.5} T^b$), four are second-order in density ($\Lambda_2 \propto \rho^2 T^b$), and one corresponds to cyclotron cooling ($\Lambda_2 \propto \rho^{0.15} T^{2.5}$). For each choice of cooling processes, the relative efficiency of the second cooling process, $\epsilon_s$ is varied.

In the case of the bremsstrahlung-dominated shock, higher harmonics are more unstable to oscillations, and this behaviour appears as a general trend in all observed cases. Increasing the efficiency of the second cooling process $\epsilon_s$ stabilizes each of the modes at a different rate, depending on the indices of the stabilizing cooling process. In most systems, sufficiently high $\epsilon_s$ causes some particular modes to be less stable than the next higher harmonic. Cases exist where a mode $n$ is unstable while harmonic $n + 1$ is stable, and successive modes are unstable again. It follows that when cooling processes with stabilizing and destabilizing tendencies compete, the oscillatory instability of one mode does not necessarily imply the instability of all higher modes.

The dimensionless eigenfrequencies $\delta_I$ constitute a sequence which resembles the modes of a pipe open at one end: $\delta_I \approx \delta_{IO}(n - 1/2) + \delta_C$. The frequency spacing constant of the modes, $\delta_{IO}$, diminishes as the stabilizing cooling process becomes important. This follows nearly identical functions in $\epsilon_s$, except for the cases when temperature dependence is weaker than the density dependence, where the reduction is more gradual. The offset $\delta_C$ is small and negative for low $\epsilon_s$, and in most cases it increases with the efficiency of the stabilizing process. In cases with high temperature and density power dependence, $\delta_C$ reaches a maximum and then decreases again for larger $\epsilon_s$.

## ACKNOWLEDGMENTS

## REFERENCES

Aizu K., 1973, Prog. Theor. Phys., 49, 1184
Bertschinger E., 1986, ApJ, 304, 154
Chanmugam G., Langer S. H., Shaviv G., 1985, ApJ, 299, L87
Chevalier R. A., Imamura J. N., 1982, ApJ, 261, 543
Cropper M., 1990, Space Sci. Rev., 54, 195
Dgani R., Soker N., 1994, ApJ, 434, 262
Gaetz T. J., Edgar R. J., Chevalier R. A., 1988, ApJ, 329, 927
Falle S. A. E. G, 1975, MNRAS, 172, 55
Falle S. A. E. G, 1981, MNRAS, 195, 1011
Houck J. C., Chevalier R. A., 1992, ApJ, 395, 592
Imamura J. N., 1985, ApJ, 296, 128
Imamura J. N., Wolff M. T., 1990, ApJ, 355, 216
Imamura J. N., Wolff M. T., Durisen R. H., 1984, ApJ, 276, 667
Imamura J. N., Aboasha A., Wolff M. T., Wood K. S., 1996, ApJ, 458, 327
Innes D. E., Giddings J. R., Falle S. A. E. G., 1987a, MNRAS, 224, 179
Innes D. E., Giddings J. R., Falle S. A. E. G., 1987b, MNRAS, 226, 67
King A. R., Lasota J. P., 1979, MNRAS, 188, 653
Lamb D. Q., Masters A. R., 1979, ApJ, 234, L117
Langer S. H., Chanmugam G., Shaviv G., 1981, ApJ, 245, L23
Langer S. H., Chanmugam G., Shaviv G., 1982, ApJ, 258, 289
Rybicki G. B., Lightman A. P., 1979, Radiative Processes in Astrophysics. John Wiley & Sons, New York
Saxton C. J., Wu K., Pongracic H., 1997, Publ. Astron. Soc. Aust., 14, 164
Tóth G., Draine B. T., 1993, ApJ, 413, 176
Warner B., 1995, Cataclysmic Variable Stars. Cambridge Univ. Press, Cambridge
Wolff M. T., Gardner J., Wood K. S., 1989, ApJ, 346, 833
Wu K., 1994, Proc. Astron. Soc. Aust., 11, 61
Wu K., Chanmugam G., Shaviv G., 1992, ApJ, 397, 232
Wu K., Chanmugam G., Shaviv G., 1994, ApJ, 426, 664
Wu K., Pongracic H., Chanmugam G., Shaviv G., 1996, Publ. Astron. Soc. Aust., 13, 93

## APPENDIX A:   FINDING THE EIGENFREQUENCIES

Values of the perturbed variables at the shock ($\tau = 1/4$) are completely determined by the Rankine–Hugoniot strong shock jump conditions: $\zeta_R = \zeta_I = 0$, $\pi_R = 3/2$, $\pi_I = 0$, $\eta_R = 3/4$, $\eta_I = 0$. (See the appendix in Saxton et al. 1997 for a derivation.) The differential equations are integrated with respect to the dimensionless velocity from the shock down to the fixed wall surface ($\tau = 0$), where only two boundary conditions apply. These conditions state that both the real and imaginary parts of the perturbed velocity vanish at the surface: $\eta_R = \eta_I = 0$.

The method for finding the oscillatory modes relies on these conditions. A grid of points is chosen in a rectangular region of the complex $\delta$-eigenplane, and the equations are integrated at each point. The value of $1/|\eta|$ is plotted over the grid. In the neighbourhood of the eigenvalues this number becomes large, appearing as a sharp spike on the surface plot of $1/|\eta|$ (see Fig. A1).

To obtain the eigenvalues, we select a small rectangular area around one of these spikes and evaluate $1/|\eta|$ over a 64-point grid. The grid point where this is maximum is then chosen as the centre of a smaller grid, and the process is iterated until the width of the search area is smaller than a desired precision.
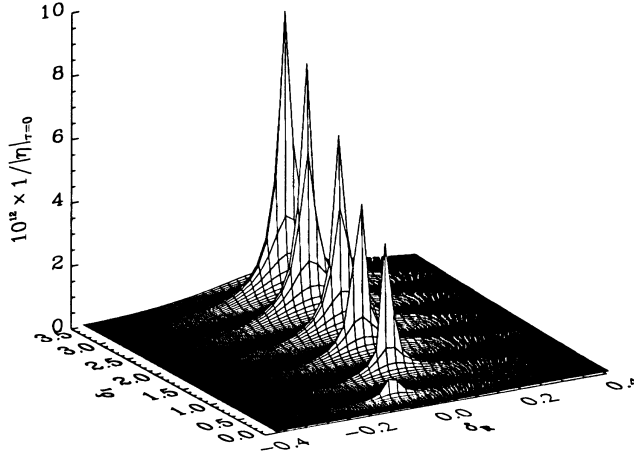


**Figure A1.** $1/|\eta|$ evaluated at the stationary (lower) boundary, $\tau = 0$, plotted in the eigenplane of complex dimensionless frequency ($\delta$). The complex dimensionless perturbed velocity is $\eta$. Its units in this plot are arbitrary. The spikes are indefinitely tall at the exact eigenvalues; the height in surrounding areas depends on proximity to the eigenvalues.

## APPENDIX B:   LINEAR FIT TO THE EIGENFREQUENCIES

The imaginary part of the eigenvalue ($\delta_I$), which is a scaled oscillation frequency for the mode, is approximately quantized like the modes of a pipe open at one end:

$$\delta_I \approx \delta_{IO}(n - 1/2) + \delta_C. \tag{B1}$$

The parameters $\delta_{IO}$ and $\delta_C$ are respectively the frequency spacing of the modes, and a small constant offset to the sequence. Their values depend upon the power-law indices ($\alpha,\beta$) and the relative efficiency of the second cooling process ($\epsilon_s$). The variation of mode spacing and offset for the various power laws is illustrated in Figs B1–B8.
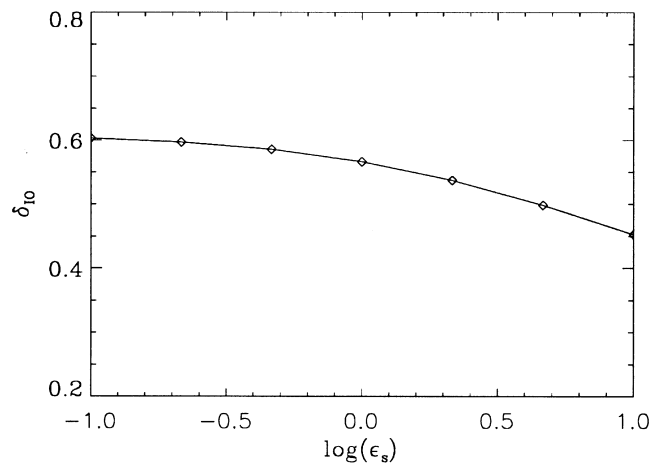


**Figure B1.** Variation of the modal frequency spacing $\delta_{IO}$ with efficiency of the second cooling function for cyclotron cooling power-law ($\alpha = 2.0, \beta = 3.85$).
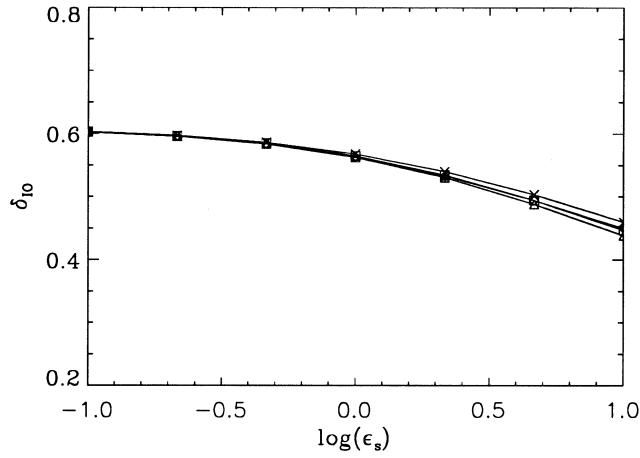
**Figure B2.** Variation of the modal frequency spacing $\delta_{IO}$ with efficiency of the second cooling function for cooling power-law indices $\alpha = 0.5, 1.5, 2.5$ and $3.5$, and $\beta = \alpha + 1$, respectively marked by diamonds ($\lozenge$), triangles ($\triangle$), squares ($\square$) and crosses ($\times$).
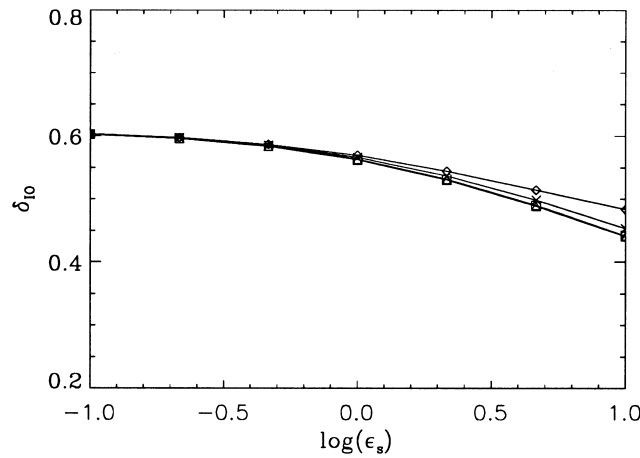


**Figure B3.** Variation of the modal frequency spacing $\delta_{IO}$ with efficiency of the second cooling function for cooling power-law indices $\alpha = 0.5, 1.5, 2.5$ and $3.5$, and $\beta = \alpha + 0.5$, respectively marked by diamonds ($\lozenge$), triangles ($\triangle$), squares ($\square$) and crosses ($\times$).
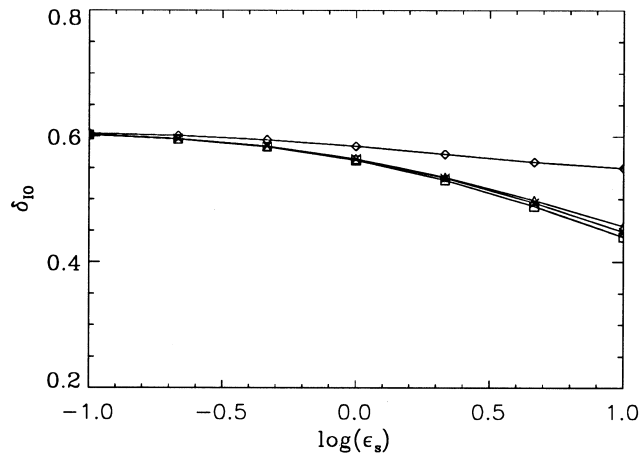


**Figure B4.** Variation of the modal frequency spacing $\delta_{IO}$ with efficiency of the second cooling function for cooling power-law indices $\alpha = 0.5, 1.5, 2.5$ and $3.5$, and $\beta = \alpha$, respectively marked by diamonds ($\lozenge$), triangles ($\triangle$), squares ($\square$) and crosses ($\times$).
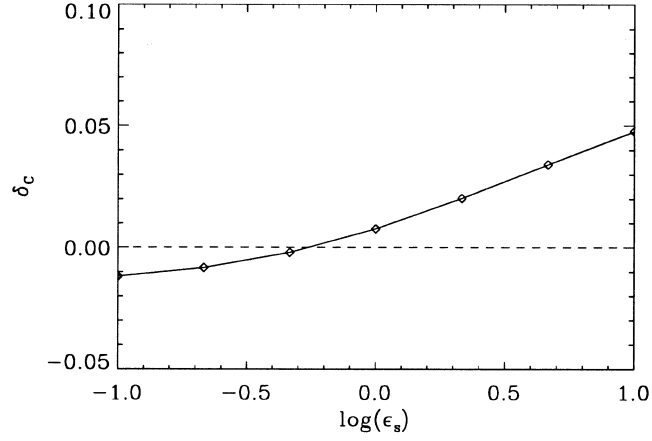
**Figure B5.** Variation of the frequency offset term $\delta_C$ with efficiency of the second cooling function for cyclotron cooling power-law ($\alpha = 2.0, \beta = 3.85$).
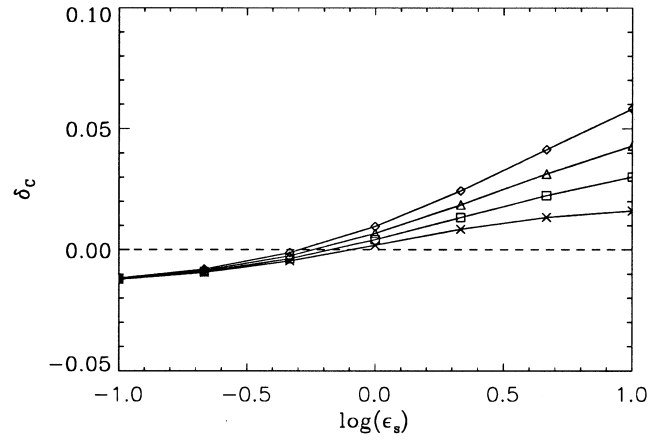


**Figure B6.** Variation of the frequency offset term $\delta_C$ with efficiency of the second cooling function for cooling power-law indices $\alpha = 0.5, 1.5, 2.5$ and $3.5$, and $\beta = \alpha + 1$, respectively marked by diamonds ($\lozenge$), triangles ($\triangle$), squares ($\square$) and crosses ($\times$).
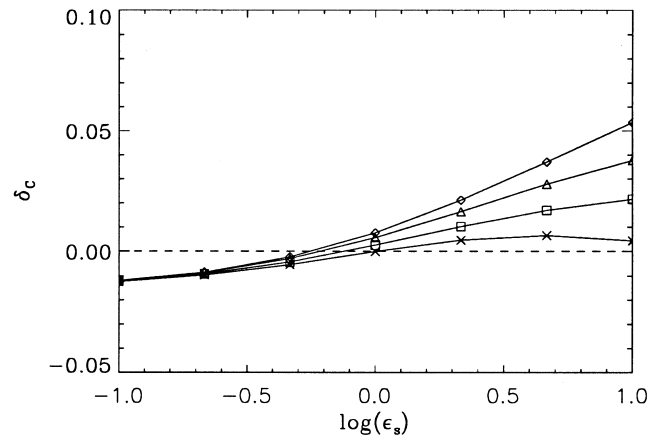


**Figure B7.** Variation of the frequency offset term $\delta_C$ with efficiency of the second cooling function for cooling power-law indices $\alpha = 0.5, 1.5, 2.5$ and $3.5$, and $\beta = \alpha + 0.5$, respectively marked by diamonds ($\lozenge$), triangles ($\triangle$), squares ($\square$) and crosses ($\times$).
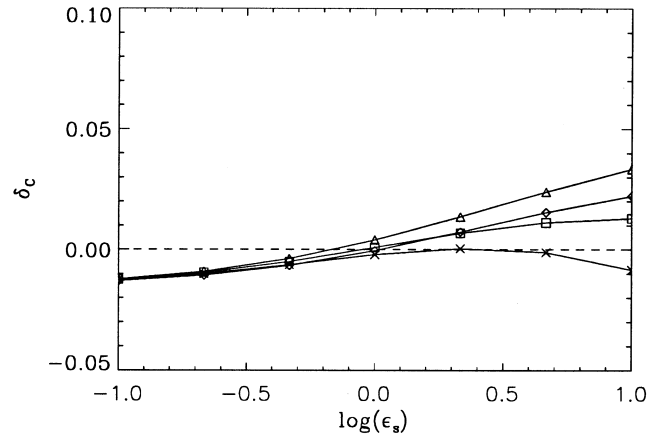
**Figure B8.** Variation of the frequency offset term $\delta_C$ with efficiency of the second cooling function for cooling power-law indices $\alpha = 0.5, 1.5, 2.5$ and $3.5$ and $\beta = \alpha$, respectively marked by diamonds ($\lozenge$), triangles ($\triangle$), squares ($\square$) and crosses ($\times$).

This paper has been typeset from a $T_EX/L^AT_EX$ file prepared by the author.